Chapter 1

The Assessment of Land Degradation and Desertification in Mexico: Mapping Regional Trend Indicators with Satellite Data

Martin Enrique Romero-Sanchez,
Antonio Gonzalez-Hernandez and
Francisco Moreno-Sanchez

Additional information is available at the end of the chapter

http://dx.doi.org/10.5772/64241

Abstract

Understanding the patterns of land degradation and desertification to develop mitigation strategies requires identification of methods for accurate and spatially explicit assessment and monitoring. Remote sensing data offer the possibility to develop strategies that outline degradation and desertification. The free access policy on satellite imagery enables a new pathway to measure, assess, and monitor land degradation using indicators derived from multispectral satellite data. This chapter seeks to explore a methodology for land degradation and desertification assessment and monitoring, based on freely available multispectral satellite data. The method identifies net primary productivity (NPP) and canopy cover (CC) as indicators of degradation. The trajectories of these indicators show patterns and trends over time. The methodological development presented here is intended to be a tool for regional landscape monitoring and assessment, enabling the formulation of corrective action plans. This methodology was tested in a semi-deciduous ecosystem in the southeast of Mexico.

Keywords: land degradation, desertification, satellite data, assessment, monitoring

1. Introduction

Land degradation and desertification not only contribute to the effects of climate change but also to the loss of productivity, biodiversity, and functionality of forest landscapes. Land use

change and associated processes are responsible for around 10% of net global carbon emissions[1]. Land degradation and desertification understood as the loss of productive capacity of the land [1] affect ecosystem productivity, socioeconomic problems, and food security. The UnitedNations through the United Nations Convention to Combat Desertification (UNCCD) seeks to identify and define strategies that support sustainable regional development to reverse and prevent desertification and land degradation. The UNCCD works to help countries to improve living conditions of people in drylands and to maintain and restore land and soil productivity.

One of the main issues in the land degradation and desertification programs is the requirement of robust methods to quantify degradation [2]. The fundamental challenge is providing a reliable account of it, and remote sensor techniques should be reliable and continuous to be a source of information [3–5]. To develop a regional and local mechanism to reverse and prevent degradation, it is imperative then to define monitoring and assessing strategies. The constant and exponential increase of remote sensing technologies offers different options to evaluate phenomena such as land degradation. Organizations dedicated to the production of new remote sensing technologies have implemented new satellite sensors with higher spatial resolution (e.g. IKONOS-2, QuickBird-2,SPOT-5) which indicates a new age of terrestrial observation and digital mapping [2, 6–9].

Satellite imagery has been taking information from the Earth's surface for last 40 years in a continuous and reliable way (i.e. Landsat program). Multispectral satellite imagery such as Landsat has opened new avenues for understanding ecological and land cover dynamics [10]. Landsat mission has been collecting imagery since 1972, providing a record of the status and dynamics of the Earth [11, 12]. Changes to policy data in 2008 make free and available the Landsat archive to any user [13]. The free distribution policy increased the supply of imagery dramatically; thus, the use and analysis of the Landsat archive have increased the opportunities to research in a variety of disciplines [10].

Optical remote sensing has been improved by spatial resolution (pixel size), spectral resolution (number of wavebands), radiometric resolution (sensibility to detect radiation changes), and temporal resolution (data acquisition frequency), which means getting capabilities of measurement in quasi-real-time [14–17]. This scenario opens up the possibility to implement powerful monitoring strategies by taking advantage of the free database policies that many entities have today. Mexico is the perfect example; almost all spatial information is freely available through different government websites. Therefore, some indicators related to degradation are available to be estimated by using remote sensing and ground data. The symbols used are capable, through trajectory or time series analysis, of detecting and mapping out changes over time.

The chapter examines the capabilities of freely available remote sensing, combined with field data, in deriving some degradation indicators. The main idea is the construction of a platform for regional land degradation monitoring and assessment. One of the main assumptions of

[1] IPCC (2013) Intergovernmental Panel on Climate Change. The Physical Science Basis. Contribution of Working Group I to the Fifth Assessment Report of the Intergovernmental Panel on Climate Change.

http://dx.doi.org/10.5772/64241

this approach is that it can be replicated in different regions of the developing world. Additionally, the cost of applications is minimal if remote sensing and field data are available.

2. Assessment of land degradation and desertification approaches

Land degradation, as has been pointed out by the UNCDD, is a global development and environment issue that affects mostly developing countries regarding the economic impact and food security [18]. The assessment and monitoring frameworks developed to provide information about land degradation have been very valuable; however, there are some opportunities to improve and test methodologies according to regional and country needs.

Land degradation and desertification are concepts that are strongly related. Land degradation can be defined as the loss or reduction of the biological production of farmlands, grasslands, forests, and wooded areas and is the result of intense land use or a process (or a combination of the process), including those coming from human actions. It is the outcome of the mismatch between land quality and the intensity of activity part of the actual land use.

According to the UNCCD, land degradation is a complex set of processes of the impoverishment of terrestrial ecosystem, either natural or human-induced, that causes the land to be no longer able to sustain its economic functions or the original ecological functions correctly [18]. The consequences of land degradation are land productivity reduction, socio-economic problems, including uncertainty in food security, migration, and damage to ecosystems.

Desertification, on the other hand, is defined as land degradation occurring in arid-semiarid and dry sub-humid areas caused by a combination of climatic factors and human activities. Therefore, only land degradation occurring in drylands is considered as part of a desertification process [19]. As many climatic scenarios have to point out, many areas across the world are vulnerable to climate change because it is going to accelerate the degradation process.

2.1. The global assessment of human-induced soil degradation (GLASOD)

This project was one of the first attempts to assess the state of degradation of soil from a global perspective [20]. The world map produced by GLASOD showed the status of human-induced soil degradation and was based mainly on expert judgment and reported degrees of land degradation that also included the notion of resilience, which was deemed essential for land management decisions. Although the GLASOD project had some criticism about the methods used, it was the only global assessment available to scientists, decision-makers, and land managers to date [18].

2.2. Land degradation assessment in drylands (LADA)

The LADA approach was developed based on the assumption that human activities on the land are the main drivers causing land degradation [21]. Therefore, defining and mapping of different land use systems are very crucial activities for underpinning the assessment and its implementation. The entire LADA approach gives consideration to the relationships between

the causes and effects that lead to degradation. The LADA project operates by using a variety of technologies, from satellite images to digital databases, to soil and vegetation sampling, and the examination of the linkages between both biophysical and socio-economic issues. Global assessment efforts list net primary productivity (NPP), rainfall use efficiency (RUE), aridity index (AI), rainfall variability (RV), and erosion risk (ER) as the leading indicators of land degradation [20].

The global land degradation assessment (GLADA) was the global component of LADA. GLADA aims at providing a baseline for the assessment of global trends in land degradation using a range of scale-appropriate indicators, many of which are collected through satellite sensors and processing satellite data and existing global databases.

2.3. Remote sensing as a tool for land degradation and desertification assessments

Methods for monitoring current state and changes of landscapes use the advantages and potential of satellite-borne or airborne remote sensing imagery. Most work has focused on identifying the change in detection of decreases in land cover rather than identifying the inversed process [22]. Considerable amount of studies explore the capabilities of remote sensing on different monitoring applications and different remote sensing approaches and data [17, 23–26].

Remote sensing applications can be summarized mainly in four categories that include: cover classification, estimation of structures, change detection, and modeling [27]. Remote sensing has the potential to be decidedly instrumental in the assessment of degradation processes at a much lower cost than any other method [28, 29]. Assessment (i.e. measurement) and monitoring through remote sensing offer a series of advantages such as consistency of data, fairly near real-time reporting, and a source for having spatially explicit data [30].

Although there are several approaches to describe land cover changes using remote sensing technology, forest inventory and limited sampling of degradation on the ground are fundamental to its quantification [31–36]. The methods used are unique to each location and strongly dependent on how its components are clearly identified and responsive to accurate measurement, and how country requirements apply to these methods.

Remote sensing is a suitable tool for the estimation of biomass for large areas, usually at regional or national scales, where field data are scarce [34]. There is an abundance of literature that describes the virtues and capabilities of remote sensing-based methods for forest monitoring assessments [17, 22, 23, 37]. The continuing advances in remote sensing science and technology and the enormous amount of data these platforms and sensors produce daily provide a promising foundation to underpin any degradation monitoring program.

The possibility of integration of optical and multispectral remote sensing data to active sensors such as LiDAR (light detection and ranging) and RADAR (radio detection and ranging), combined with ground data, has gained a significant relevance and a high potential for contributing to the design of degradation assessment and monitoring methodologies.

http://dx.doi.org/10.5772/64241

Direct detection of degradation processes, for example in forest landscapes, relates area changes to, and focuses on, forest canopy damage. These changes in forest attributes occurring during a period of time can be detected using information from natural forest resources inventories (FRI) and some from remote sensing [23, 30, 38]. Medium spatial resolution satellite remote sensing data such as Landsat Thematic Mapper (TM) and SPOT have proven capable of obtaining regional-scale forest variables [39]. Indirect approaches focus on the spatial distribution and the effects that the evolution of human infrastructure has had on the degradation of nearby areas. Often, these "indirect" factors are used as "proxies" for newly degraded areas.

3. Methodology

3.1. Mapping regional trend indicators with satellite data

Any operational monitoring assessment needs to establish as starting a clear understanding of what are the relevant and regionally significant indicators that are used as components of the analysis. This is followed by what will be the practical impact of the utilization of these parameters in the actual implementation of measuring and monitoring methods. Part of the methodological approach presented here was developed by the first author during his doctoral program and was focused on forest degradation. However, the main components were translated to the land degradation and desertification monitoring requirements as both phenomena are intimately linked.

Within the UNCCD, it is necessary to understand what are the drivers and activities causing degradation [30]. According to project needs and based on the literature reviewed, canopy cover and net primary productivity are considered as the leading indicators within this methodological framework. These variables are thus proposed as indicators of degradation (mainly forest landscapes) in practice. Although it is acknowledged that other indicators (biodiversity, disturbances, and fragmentation) are also variables that may merit to be considered, together with those above, as indicators of degradation, are not regarded as part of this chapter. However, the limitations of time and the scope of a rapid assessment do not stretch to encompass them in this study.

3.1.1. Proposed indicators

3.1.1.1. Canopy cover

Canopy cover is recognized as a significant biophysical and structural attribute of the forest [40]. It affects terrestrial energy and water exchanges, photosynthesis and transpiration, net primary production, and carbon and nutrient fluxes, and is the key element for defining forests in international and national accords [41]. Canopy cover provides an attribute that is measurable and can be used to monitor and retrieve site-specific histories of different stages within the forest landscape dynamics [41].

Canopy cover has already been used as an indicator to monitor and map forest degradation in various contexts [32, 35]. Some studies [42] evaluated forest degradation based on canopy closure classes, namely non-degraded (>70%), moderately degraded (40–70%), degraded (10–40%), and severely degraded (<10%). Another study [43] assessed forest degradation using canopy disturbance as a result of gaps produced by logging, road construction, and skid trails as an indication of forest degradation. Another approach suggested for mapping forest degradation and deforestation was the use of canopy cover combined with spectral mixture analysis, normalized difference fraction index, and a decision tree classification [44].

3.1.1.2. Net primary productivity

NPP determines the rate of atmospheric carbon sequestration and storage by vegetation [45, 46]. NPP has been used previously as an indicator of ecosystems' decline [47–49]. These approaches open the door to the possibility of using NPP as both a baseline and indicator of forest degradation [50], based on the assumptions that losses of canopy cover will affect the capacity of the forest to fix carbon and reduce NPP rates.

NPP estimations are regularly based on the light use efficiency (LUE) theory [51]. The LUE theory is estimated on two broad assumptions. First, NPP is related to the absorbed photosynthetically active radiation, APAR, where LUE determines the amount of dry matter produced per unit of APAR. Second, environmental stresses such as low temperature or water shortage have an adverse impact over LUE [52, 53]. Production efficiency models (PEM) are developed from the LUE theory. They require inputs of meteorological data and take advantage of available satellite data to derive the fraction of absorbed photosynthetically active radiation, fPAR [53]. Examples of production efficiency models include the CASA model (Carnegie-Ames-Stanford approach) [54], C-Fix [55–57], and MOD17 [48] used for monitoring NPP at regional and global scale from satellite remote sensing data.

Net primary productivity is employed by the global land degradation assessment in Drylands (LADA) project [21], where NPP is highly relevant to the assessment of degradation. NPP can be readily used as a direct indicator of the condition and trend of changes in the state of ecosystems over time, whereby the decrease in NPP over time would signal the degradation of ecosystems. Through the LADA project conducted by the FAO [18] and within the UNCCD framework [58], mapped out land degradation at national, regional, and local scales in Ethiopia using NPP as one of the major indicators in their studies.

3.1.2. Trajectory analysis and change detection

One of the most frequent uses of remote sensing is change detection [59]. The stock pile of optical satellite imagery freely available (e.g. Landsat program) [13] offers opportunities for the reconstruction and understanding of landscape dynamics. Direct comparison of pairs of images (bi-temporal analysis) is perhaps the most common approach to change detection [60].

Although many change detection methods have been developed [61–63], the question of how to reliably map land-use change remains a central challenge. Land-use change (LUC) can result

http://dx.doi.org/10.5772/64241

in both land cover conversions and land cover modifications, but remote sensing mainly focuses on mapping the former. However, land cover changes may be more prevalent, meaningful, and significant to forest degradation than conversions. Forest degradation is more likely to be the reflection of a land cover change with its particular degree of intensity and duration.

Temporal trajectory analysis is understood in this context as the analysis of the sequence of changes in detection in every pixel of the image part of a stock pile of imagery over a continuous timescale. This type of analysis has been shown particularly useful in characterizing land ecosystem dynamics since it exploits the multi-temporal sequence of images to reveal temporal patterns over several temporal scales [62, 64, 65].

Trajectory analysis from multispectral and optical remote sensing is commonly employed for detecting changes of a set of forest degradation indicator variables over time that can be readily computed from satellite images and that are associated with the state and condition of forests [66, 67].

Examples from the literature have proved the value of the trajectory analysis in forest assessments, especially those that take advantage of the stock pile of Landsat imagery [61, 68, 69]. This methodology incorporates this type of analysis as a part of the degradation assessment.

3.1.2.1. Bi-temporal analysis

The bi-temporal analysis is perhaps the most used method to perform change detection on remote sensing satellite imagery [70]. The bi-temporal change detection methods range from simple image differencing methods to statistically based methods [71]. Change detection methods have been widely used to identify changes in classes (e.g. land cover classification) or the difference between a pair of images (image differencing) [70].

3.2. Land degradation and desertification in Mexico

Mexico has the compromise to present a national report about land degradation and desertification before the UNCDD. According to official reports, 90.7% of land in the country suffers some degree of degradation [72]. On the other hand, desertification affects almost 60% of the land in the country. Degradation and desertification processes in Mexico are complex issues related to poverty and sustainability, and they are affecting all the ecosystems within the country.

3.2.1. Study area: Yucatan Peninsula, Mexico

Mexico, within its ecological and climatic conditions, offers an excellent site for experimentation and application of this methodology. Although the method can be implemented in any part of the country, it has been decided to use a region from the southeast of Mexico, in the Yucatan Peninsula as the experimental site.

The methodological framework for land degradation assessment in drylands [21] is used to support methods to evaluate degradation within a tropical dry forest area located in the

Yucatan peninsula, Mexico. Landsat imagery was used as the main source to estimate indicators such as canopy cover (CC) and net primary productivity (NPP). Use of Landsat imagery enables to see changes over time [68] within a pixel 30 m resolution over 28 years (1986–2014). The methods enabled selection of priority areas and spatial patterns. The MENDA-1 watershed [73] in the Yucatan Peninsula, Mexico, was selected as experimental area (**Figure 1**).

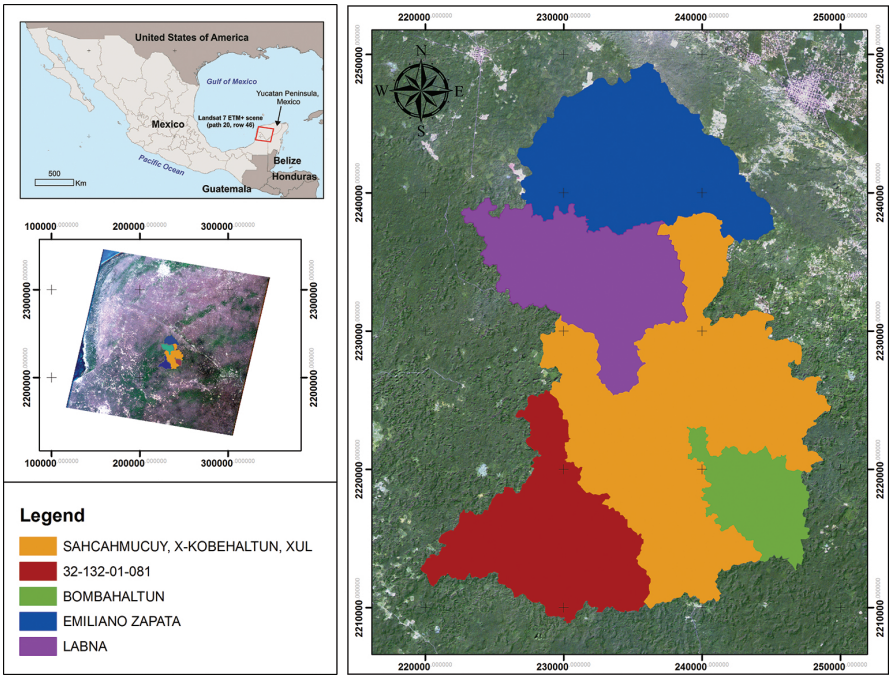

Figure 1. Study area.

The integration of the methodology is described as follows:

Selection of the indicators to monitor and assess degradation was the first step. Each one of the indicators selected was estimated using remote sensing as the primary source of data input. Because of the characteristics and free availability of Landsat archive [13], Landsat imagery is suggested as the major contribution. The indicators were estimated for the period of time required according to particular needs. Although in many tropical regions cloud cover is a significant issue, the probability of acquiring at least one cloud-free or reasonably cloud-free Landsat image per season is relatively high [74]. At least one Landsat image per season ensures continuity in historical estimations of the forest landscape dynamics based on Landsat archive.

Very high-resolution satellite imagery or LiDAR data is recommended as auxiliary data to validate calculations. Another data set crucial for the implementation of this framework was forest inventory databases. Many developing countries (e.g. Mexico) carried out periodical

http://dx.doi.org/10.5772/64241

forest inventories on a regional scale. Forest inventory data were the base for knowing the actual state of the forest and natural resources.

Once each one of the indicators has been calculated, the selection of a strategy for monitoring changes has to be made. As described before, the methods for change detection can be a time series approach (in the case of high frequency of data) or a bi-temporal change detection approach (in the case of low frequency of data). The implementation of this step allows identifying spatial and temporal patterns of the indicators used.

The establishment of a baseline and the definition of the threshold for comparisons was the next step toward the final integration. This was done using field data or high-resolution auxiliary imagery available (e.g. Google Earth™). The comparison of the spatial and temporal trends in the baseline scenario allowed identification of degraded areas regarding the indicators used.

3.2.2. Data preparation

3.2.2.1. Landsat ecosystem disturbance adaptive processing system

Landsat enhanced thematic mapper and thematic sensors imagery was used as the primary source of information. The images were obtained from the USGS website (http://glovis.usgs.gov). In the study area, like other tropical regions, cloud cover limited the choice of imagery available per year. In total, 155 Landsat scenes were downloaded. The images were in L1T geometrically corrected format and atmospherically corrected using the 6S radiative transfer approach [75].

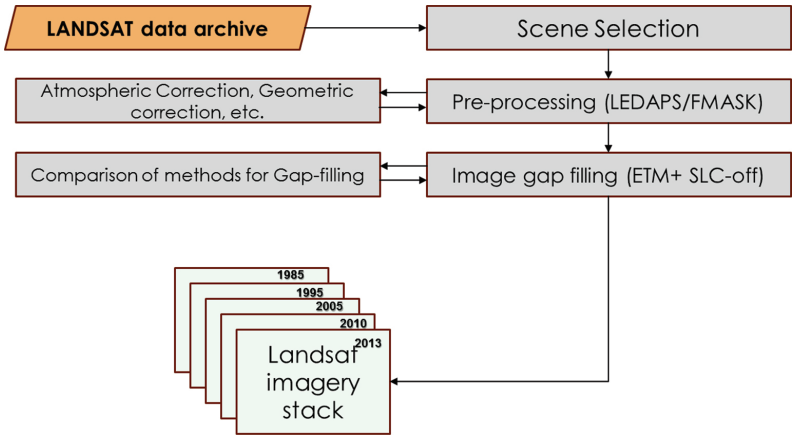

Figure 2. Satellite data preparation flow.

Landsat 7 ETM+ images acquired with the SLC-off (i.e., SLC failure in 2003) were adjusted using the algorithm Geostatistical Neighbor Spatial Pixel Interpolator, GNSPI [76]. The GNSPI

can recover efficiently the pixels missing due to SLC failure, and its outputs are suitable for forest monitoring applications [77]. Landsat imagery was separated according to the date taken (i.e. wet or dry season), and an initial cloud filter was applied. Imagery with more than 10% of cloud cover was avoided for the analysis to focus on high-quality imagery (cloud free). **Figure 2** shows in a very generic way the pre-processing process.

3.2.3. Forest degradation indicators estimation

3.2.3.1. Canopy cover

The CLASlite™ image processing system [78] was used to develop the fractional cover and forest cover maps for the Landsat dates. CLASlite™ produces photosynthetic vegetation, non-photosynthetic vegetation and, bare soil layers from the core process within CLASLite™ called Automated Monte Carlo Unmixed Process (AutoMCU). These outputs provide a quantitative analysis of the fractional or percentage cover (0–100%) of live and dead vegetation, and bare substrate within each Landsat pixel [78]. The Auto MCU submodel is based on a probabilistic algorithm designed for savanna, woodland, and shrubland ecosystems, and later modified for the tropical forest [79, 80].

Photosynthetic vegetation layers (0–100%) were used as an equivalent of field forest cover (0–100%) for subsequent analysis. To validate this assumption, the direct relationship between the PV and CC was measured. Canopy cover derived from LiDAR data was used to support the PV layers. CC LiDAR was estimated using the ratio of the pulse returned from the upper layer of tree crown (sum of all pulses > pre-defined threshold) to total returns. Hence

$$CC = \frac{nh}{n} \tag{1}$$

where

CC: canopy cover

nh: ∑all returns > predefined height

n: total returns.

The predefined height was set to 1.5 m. Range between 1.0 and 2.0 m is appropriate and has no substantial variation in the correlation between canopy cover measured in the field and the one estimated from Lidar data [81, 82].

Validation of the estimated Landsat CC was achieved by computing a residual mean of squares (RMS) of differences between Landsat CC and the Lidar CC product. This comparison was made possible by aggregating Lidar CC to 30 m to correspond to Landsat products spatially.

NPP in this study was calculated according to the theory of light use efficiency (LUE) as follows [46, 83]:

http://dx.doi.org/10.5772/64241

$$NPP = \varepsilon \cdot fPAR \cdot PAR \tag{2}$$

where

PAR is photosynthetically active radiation (MJ/(m^2 month))

fPAR is the fraction of PAR absorbed by vegetation canopy,

ε is the light use efficiency coefficient (g of C/MJ) and includes the plant respiration costs [84].

The light use efficient coefficient ε was derived following the MODIS-GPP approach [85] where ε is calculated using two factors: the biome-specific maximum conversion efficiency ε_{max}, and the effect of temperature *f(T)* and water on plant photosynthesis *f(W)* [83]. The ε_{max} used in this study was 1.044 g of C/MJ according to the lookup tables [84].

f(T) was estimated on a monthly basis using the equation developed for the terrestrial ecosystem model (TEM) [86], as:

$$f(T) = \frac{(T - Tmin)(T - Tmax)}{(T - Tmin)(T - Tmax) - (T - Topt)^2} \tag{3}$$

where *T* is the atmospheric temperature (°C); and *Tmin, Tmax*, and *Topt* are the minimum, maximum, and optimal temperatures for photosynthetic activities, respectively. Values of 2°C, 39°C, and 26°C were used for *Tmin, Tmax*, and *Topt*, respectively [47, 87].

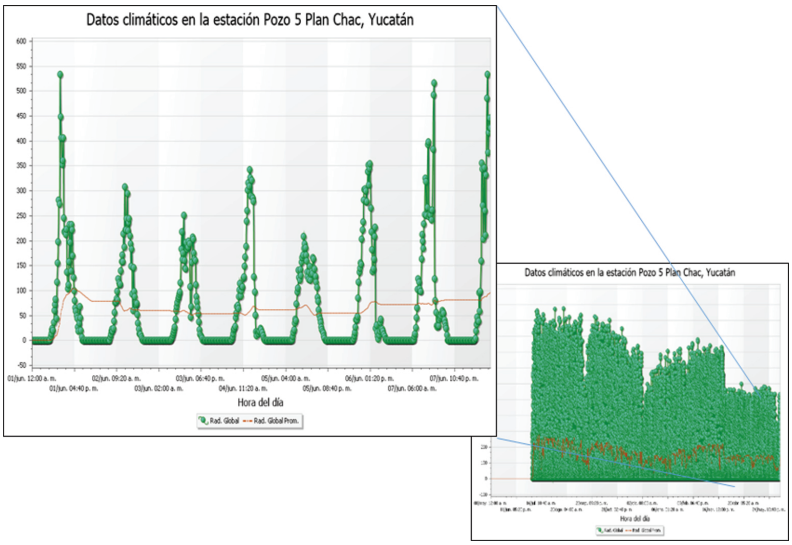

Figure 3. Daily solar radiation from the meteorological network (www.inifap.gob.mx).

The effect of water on plant photosynthesis *f(W)* was derived according to the algorithm suggested by Xiao et al. [88].

$$f(W) = \frac{1 + LSWI}{1 + LSWI_{\max}} \tag{4}$$

$$LSWI = \frac{\rho_{nir} - \rho_{swir}}{\rho_{nir} + \rho_{swir}} \tag{5}$$

where *LSWI* is the land surface water index, and $LSWI_{max}$ is the maximum *LSWI* within the plant growing season. ρ_{nir} and ρ_{swir} are the surface reflectance of the NIR and MIR bands in Landsat ETM+ images.

Meteorological data from the national meteorological network from the National Institute of Forestry, Agriculture, and Livestock Research (INIFAP) were used as inputs for the NPP calculations (**Figure 3**).

3.2.4. Trajectory analysis

Trajectory analysis and change detection on degradation indicators were performed using two different approaches: a time series and a bi-temporal approach. The BFAST [63] model was selected as the time series analysis approach. Canopy cover was the only indicator that went into the BFAST time series analysis because of the high frequency of data available. Change detection on above-ground biomass and NPP were performed using a bi-temporal approach as a result of the low frequency in data available. Next, the implementation of both methods is described.

3.2.4.1. BFAST

The BFAST and BFAST monitor algorithms were applied as a trajectory analysis strategy. Canopy cover derived from Landsat from the period 1988 to 2014 was used to implement the time series analysis. The algorithms were implemented using the BfastSpatial package for R software available at http://github.com/dutri001/bfastSpatial [64, 89]. The steps followed to implement BfastSpatial were (a) pre-processing of surface reflectance data, (b) inventorying and preparing data for analysis, and (c) analysis and formatting of change detection results.

3.2.4.2. Bi-temporal change detection

Change detection on a bi-temporal basis was implemented in NPP layers. The imaging differencing method allowed direct comparison between images and was used for two reasons: it is straightforward and allows an easy interpretation of the results [70]. The image differencing method consisted of precisely co-registered multi-temporal images used to produce a residual image to represent changes. Although the USGS service provides Landsat imagery as

http://dx.doi.org/10.5772/64241

LT1 (geometrically corrected), an automatic image registration was performed for every change detection process.

The difference between layers was measured directly from values of the pixel image. The expression of image differencing is as follows:

$$I_d(x,y) = I_1(x,y) - I_2(x,y) \tag{6}$$

where I_1 and I_2 are images from time t_1 and t_2, (x, y) are coordinates, and I_d is the difference image. Pixels with no change were distributed around the mean while pixels with change were circulated in the tails of the distribution curve. Since change can occur in both directions, it is therefore up to the analyst to decide which image to subtract from which [90].

The image differencing method was carried out by the ENVI™ 5.2 interface. Possible inconstancies between indicators used in this process due to errors associated with estimations were minimized using a normalization process between Time 1 and Time 2 layers. This normalization process applies a gain and an offset to the Time 2 layer so that it has same mean and standard deviation as the time layer.

The next step was to select a threshold value that allows the method to identify areas that have a significant change. Otsu's auto-thresholding method [91] was used to set the threshold for identifying important changes. Otsu's is a histogram shape-based method. It is based on discriminate analysis and uses the zeroth- and the cumulative first-order moments of the histogram for calculating the value of the thresholding level.

A clean-up process was carried out where a kernel size of 3 × 3 pixels was applied to remove speckling noise, and a minimum aggregate size set to 25 was configured to remove minuscule regions.

The outputs produced by the changed detection method were (a) an image change and (b) an image difference. The latest was kept to identify "degraded" areas by applying a classification tree based on field observations and very high-resolution imagery as training sites. This approach followed the same logic described earlier to detect break points in the time series. The image change was used to determine deforestation in the study area.

3.3. Results and discussion

The procedures in this integrated methodology allowed for the identification of areas that have been degraded. The results allowed to highlight areas that have been degraded due to loss of net primary productivity and forest cover. Integration of the different elements in this methodology enabled the identification of areas that maintain a "stable" condition and areas that change over the period evaluated.

According to the results obtained here, Landsat-derived indicators (forest canopy cover and net primary productivity) showed effectiveness in the identification and mapping of degraded forest landscapes. The results of this study also suggest that it is possible to produce explicit and high-resolution canopy cover maps over relatively large areas.

The net primary productivity also showed its value in identifying and mapping forest degradation. NPP is a forest parameter that is difficult to estimate and can be subject to high levels of uncertainty [92–94]. NPP was estimated for the period 2007–2013 showing mean values in the range of 480–512 and maximum values of 742–936 gC/m^2/year. Although NPP estimations are difficult to perform and validate due to lack of field data, programs such the INIFAP meteorological network that register climatic variables every 15 minutes, and Eddy covariance tower networks along with remote sensing data, are promissory elements to support NPP modeling.

Finally, the results of the trajectory analysis of degradation indicators (NPP and CC) showed (overall timescale 28 years) a slight tendency toward forest degradation and decline, punctuated by cyclic oscillations of decline and recovery that indicate the cyclic nature of disturbances of the study area. These trends are shown in **Figure 4**.

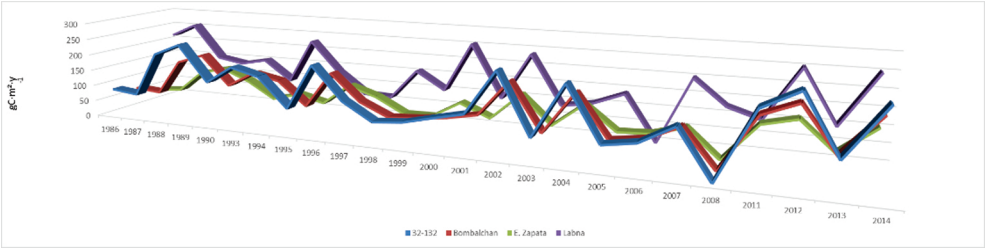

Figure 4. Trajectories of means of net primary productivity, central Yucatan, Mexico.

4. Conclusions

This chapter has shown how free remote sensing data (i.e. Landsat archive) can outline degradation by computing some indicators such as net primary productivity (NPP) and canopy cover (CC).

The key features and benefits of this methodology are (a) it is easy to implement, (b) it can be adaptable to specific site conditions, and (c) it allows an opportunity to identify regional trends by analyzing the indicators of degradation over time.

The main feature of this methodology is its suitability for use in many regions of the developing world where more sophisticated and, therefore, data-rich and demanding procedures are not possible. The trajectories of these degradation indicators can be used as a tool for regional monitoring of ecosystem condition and trends, enabling the formulation of remedial action plans.

The methodology described here also allows for the identification of the temporal and spatial distributions of forest degradation based on the indicators used.

The next steps for this methodology are:

a. To test and validate the method across the country and other regions. Partnership with the National Forestry Commission and the National Institute of Forestry, Agriculture and Livestock Research has been established.

b. To add the Eddy covariance tower network along with remote sensing data that are promissory elements to support NPP modeling in a reliable way in the country.

Acknowledgements

Acknowledgment is extended to the Mexican Council for Science and Technology (CONACyT) and the National Institute of Forestry, Agriculture and Livestock Research (INIFAP) of Mexico for funding this study.

Author details

Martin Enrique Romero-Sanchez*, Antonio Gonzalez-Hernandez and Francisco Moreno-Sanchez

*Address all correspondence to: romero.martin@inifap.gob.mx

National Institute of Forestry, Agriculture and Livestock Research, Mexico City, Mexico

References

[1] UNEP. Global Environment Outlook 3: Past, present and future perspectives. [Internet]. London, UK.: Earthscan; 2002. 34 p. Available from: http://www.unep.org/geo/geo3/english/pdfs/prelims.pdf

[2] Gonzalez P, Asner GP, Battles JJ, Lefsky MA, Waring KM, Palace M. Forest carbon densities and uncertainties from Lidar, QuickBird, and field measurements in California. Remote Sens Environ [Internet]. Elsevier Inc.; 2010 Jul [cited 2014 Jan 21];114(7): 1561–75. Available from: http://linkinghub.elsevier.com/retrieve/pii/S0034425710000702

[3] Baccini A, Laporte N, Goetz SJ, Sun M, Dong H. A first map of tropical Africa's above-ground biomass derived from satellite imagery. Environ Res Lett [Internet]. 2008 Oct 10 [cited 2014 Jan 23];3(4):045011. Available from: http://stacks.iop.org/1748-9326/3/i=4/a=045011?key=crossref.24eaa14be3435d90432b8de989ed79c3

[4] Popescu SC. Estimating biomass of individual pine trees using airborne lidar. Biomass and Bioenergy [Internet]. 2007 Sep [cited 2014 Feb 20];31(9):646–55. Available from: http://linkinghub.elsevier.com/retrieve/pii/S0961953407001316

[5] Wang G, Oyana T, Zhang M, Adu-Prah S, Zeng S, Lin H, et al. Mapping and spatial uncertainty analysis of forest vegetation carbon by combining national forest inventory data and satellite images. For Ecol Manage [Internet]. 2009 Sep [cited 2014 Feb 12]; 258(7):1275–83. Available from: http://linkinghub.elsevier.com/retrieve/pii/S0378112709004253

[6] Martinuzzi S, Gould WA, Ramos Gonzalez OM, Robles AM, Maldonado PC, Pérez-Buitrago N, et al. Mapping tropical dry forest habitats integrating Landsat NDVI, Ikonos imagery, and topographic information in the Caribbean Island of Mona. Rev Biol Trop. 2008;56(2):625–39.

[7] Castillo-Santiago MÁ, Ghilardi A, Oyama K, Hernández-Stefanoni JL, Torres I, Flamenco-Sandoval A, et al. Estimating the spatial distribution of woody biomass suitable for charcoal making from remote sensing and geostatistics in central Mexico. Energy Sustain Dev [Internet]. International Energy Initiative; 2013 Apr [cited 2014 Nov 29];17(2):177–88. Available from: http://linkinghub.elsevier.com/retrieve/pii/S0973082612000762

[8] Karl JW, Maurer BA. Multivariate correlations between imagery and field measurements across scales: comparing pixel aggregation and image segmentation. Landsc Ecol [Internet]. 2009 Dec 11 [cited 2014 Mar 23];25(4):591–605. Available from: http://link.springer.com/10.1007/s10980-009-9439-4

[9] Hu Q, Wu W, Xia T, Yu Q, Yang P, Li Z, et al. Exploring the use of google earth imagery and object-based methods in land use/cover mapping. remote sens [Internet]. 2013 Nov 15 [cited 2014 Mar 27];5(11):6026–42. Available from: http://www.mdpi.com/2072-4292/5/11/6026/

[10] Wulder MA, Masek JG, Cohen WB, Loveland TR, Woodcock CE. Opening the archive: how free data has enabled the science and monitoring promise of Landsat. Remote Sens Environ [Internet]. Elsevier B.V.; 2012 Jul [cited 2014 Apr 29];122:2–10. Available from: http://linkinghub.elsevier.com/retrieve/pii/S003442571200034X

[11] Cohen WB, Goward SN. Landsat's role in ecological applications of remote sensing. Bioscience [Internet]. 2004 [cited 2014 Apr 1];54(6):535. Available from: http://bioscience.oxfordjournals.org/content/54/6/535.full.pdf+html

[12] USGS. SLC-off gap-filled products. Gap-Fill Algorithm Methodology [Internet]. 2004. pp. 1–12. Available from: www.ga.gov.au/servlet/BigObjFileManager?bigobjid=GA4861

[13] Woodcock CE, Allen R, Anderson M, Belward A, Bindschadler R, Cohen W, et al. Free access to landsat imagery. Science [Internet]. 2008 May 23 [cited 2014 Apr 20];320(5879): 1011. Available from: http://www.ncbi.nlm.nih.gov/pubmed/18497274

[14] Roy DP, Wulder MA, Loveland TR, C.E. W, Allen RG, Anderson MC, et al. Landsat-8: science and product vision for terrestrial global change research. Remote Sens Environ [Internet]. Elsevier B.V.; 2014 Apr [cited 2014 Apr 28];145:154–72. Available from: http://linkinghub.elsevier.com/retrieve/pii/S003442571400042X

[15] Zolkos SG, Goetz SJ, Dubayah R. A meta-analysis of terrestrial aboveground biomass estimation using lidar remote sensing. Remote Sens Environ [Internet]. Elsevier Inc.; 2013 Jan [cited 2014 Mar 2];128:289–98. Available from: http://linkinghub.elsevier.com/retrieve/pii/S0034425712004051

[16] Hansen MC, Potapov P V, Moore R, Hancher M, Turubanova S a, Tyukavina a, et al. High-resolution global maps of 21st-century forest cover change. Science [Internet]. 2013 Nov 15 [cited 2014 Mar 20];342(6160):850–3. Available from: http://www.ncbi.nlm.nih.gov/pubmed/24233722

[17] Goetz SJ, Baccini A, Laporte NT, Johns T, Walker W, Kellndorfer J, et al. Mapping and monitoring carbon stocks with satellite observations: a comparison of methods. Carbon Balance Manag [Internet]. 2009 Jan [cited 2014 Feb 21];4:2. Available from: http://www.pubmedcentral.nih.gov/articlerender.fcgi?artid=2667409&tool=pmcentrez&rendertype=abstract

[18] Ahmed OS. Methodology for the assessment of the impacts of climate change on land degradation at multiple scales: use of high resolution satellite imagery, modelling, and ground measurements for the assessment in Ethiopia. Trent University: Ontario, Canada; 2012.

[19] UNCCD. Desertification: the invisible frontline. [Internet]. 2014. Available from: http://www.unccd.int/Lists/SiteDocumentLibrary/Publications/NEW_Invisible_Front_Line_ EN.pdf

[20] LADA Land Degradation Assessment in Drylands. Guidelines for the identification, selection and description of nationally based indicators of land degradation and improvement [Internet]. UNEP: Rome, Italy; 2009. p. 57. Available from: http://www.fao.org/nr/lada/index.php?option=com_content&view=article&id=152&Itemid=168&lang=en

[21] Ponce-Hernandez R, Koohafkan P. A methodology for land degradation assessment at multiple scales based on the DPSIR approach: experiences from applications to drylands. In: Zdruli P, Pagliai M, Kapur S, Faz Cano A, editors. Land Degradation and Desertification: Assessment, Mitigation and Remediation [Internet]. Dordrecht: Springer Netherlands; 2010 [cited 2014 Aug 19]. pp. 49–65. Available from: http://link.springer.com/10.1007/978-90-481-8657-0

[22] GOFC-GOLD. A sourcebook of methods and procedures for monitoring and reporting anthropogenic greenhouse gas emissions and removals caused by deforestation, gain and losses of carbon stocks in forests remaining forests, and forestation. Report Version

COP17-1. [Internet]. Alberta, Canada; 2011. Available from: http://www.gofc-gold.uni-jena.de/redd/

[23] Gibbs HK, Brown S, Niles JO, Foley Ja. Monitoring and estimating tropical forest carbon stocks: making REDD a reality. Environ Res Lett [Internet]. 2007 Oct 5 [cited 2014 Mar 22];2(4):045023. Available from: http://stacks.iop.org/1748-9326/2/i=4/a=045023?key=crossref.4118e8af5a9a3ac02c1bb32f8a92c50f

[24] Olander LP, Gibbs HK, Steininger M, Swenson JJ, Murray BC. Reference scenarios for deforestation and forest degradation in support of REDD: a review of data and methods. Environ Res Lett [Internet]. 2008 Apr 11 [cited 2014 Jan 28];3(2):025011. Available from: http://stacks.iop.org/1748-9326/3/i=2/a=025011?key=crossref.7b824939f979eb52873acc0988b80a16

[25] Asner GP, Powell GVN, Mascaro J, Knapp DE, Clark JK, Jacobson J, et al. High-resolution forest carbon stocks and emissions in the Amazon. Proc Natl Acad Sci U S A [Internet]. 2010 Sep 21 [cited 2014 Feb 21];107(38):16738–42. Available from: http://www.pubmedcentral.nih.gov/articlerender.fcgi?artid=2944749&tool=pmcentrez&rendertype=abstract

[26] Joseph S, Murthy MSR, Thomas AP. The progress on remote sensing technology in identifying tropical forest degradation: a synthesis of the present knowledge and future perspectives. Environ Earth Sci [Internet]. 2010 Dec 30 [cited 2014 Jul 23];64(3):731–41. Available from: http://link.springer.com/10.1007/s12665-010-0893-8

[27] Franklin SE. Remote sensing for sustainable forest management [Internet]. New York: Lewis; 2001. 407 p. Available from: http://www.amazon.ca/exec/obidos/redirect?tag=citeulike09-20&path=ASIN/1566703948

[28] Mascaro J, Detto M, Asner GP, Muller-Landau HC. Evaluating uncertainty in mapping forest carbon with airborne LiDAR. Remote Sens Environ [Internet]. Elsevier Inc.; 2011 Dec [cited 2014 Jan 20];115(12):3770–4. Available from: http://linkinghub.elsevier.com/retrieve/pii/S0034425711002720

[29] Olander LP, Galik CS, Kissinger GA. Operationalizing REDD+: scope of reduced emissions from deforestation and forest degradation. Curr Opin Environ Sustain [Internet]. Elsevier B.V.; 2012 Dec [cited 2014 Feb 18];4(6):661–9. Available from: http://linkinghub.elsevier.com/retrieve/pii/S1877343512000942

[30] Herold M, Román-Cuesta RM, Mollicone D, Hirata Y, Van Laake P, Asner GP, et al. Options for monitoring and estimating historical carbon emissions from forest degradation in the context of REDD+. Carbon Balance Manag [Internet]. BioMed Central Ltd; 2011 Jan [cited 2014 Mar 2];6(1):13. Available from: http://www.pubmedcentral.nih.gov/articlerender.fcgi?artid=3233497&tool=pmcentrez&rendertype=abstract

[31] Souza, Jr C, Firestone L, Moreira Silva L, Roberts D. Mapping forest degradation in the Eastern Amazon from SPOT 4 through spectral mixture models. Remote Sens Environ

[Internet]. 2003 Nov 15 [cited 2014 Nov 22];87(4):494–506. Available from: http://linkinghub.elsevier.com/retrieve/pii/S0034425703002086

[32] Panta M, Kim K, Joshi C. Temporal mapping of deforestation and forest degradation in Nepal: Applications to forest conservation. For Ecol Manage [Internet]. 2008 Oct [cited 2014 Jan 27];256(9):1587–95. Available from: http://linkinghub.elsevier.com/retrieve/pii/S0378112708005616

[33] Tang L, Shao G, Piao Z, Dai L, Jenkins MA, Wang S, et al. Forest degradation deepens around and within protected areas in East Asia. Biol Conserv [Internet]. Elsevier Ltd; 2010 May [cited 2014 Feb 6];143(5):1295–8. Available from: http://linkinghub.elsevier.com/retrieve/pii/S000632071000025X

[34] Eckert S, Ratsimba HR, Rakotondrasoa LO, Rajoelison LG, Ehrensperger A. Deforestation and forest degradation monitoring and assessment of biomass and carbon stock of lowland rainforest in the Analanjirofo region, Madagascar. For Ecol Manage [Internet]. Elsevier B.V.; 2011 Dec [cited 2014 Mar 2];262(11):1996–2007. Available from: http://linkinghub.elsevier.com/retrieve/pii/S0378112711005330

[35] Mon MS, Mizoue N, Htun NZ, Kajisa T, Yoshida S. Factors affecting deforestation and forest degradation in selectively logged production forest: a case study in Myanmar. For Ecol Manage [Internet]. Elsevier B.V.; 2012 Mar [cited 2014 Feb 21];267:190–8. Available from: http://linkinghub.elsevier.com/retrieve/pii/S0378112711007213

[36] Kronseder K, Ballhorn U, Böhm V, Siegert F. Above ground biomass estimation across forest types at different degradation levels in Central Kalimantan using LiDAR data. Int J Appl Earth Obs Geoinf [Internet]. Elsevier B.V.; 2012 Aug [cited 2014 Mar 5];18:37–48. Available from: http://linkinghub.elsevier.com/retrieve/pii/S0303243412000128

[37] Asner GP, Mascaro J. Mapping tropical forest carbon: Calibrating plot estimates to a simple LiDAR metric. Remote Sens Environ [Internet]. Elsevier Inc.; 2014 Jan [cited 2014 Jan 20];140:614–24. Available from: http://linkinghub.elsevier.com/retrieve/pii/S003442571300360X

[38] GFOI. Integrating remote-sensing and ground-based observations for estimation of emissions and removals of greenhouse gases in forests: methods and guidance from global forest observations initiative. 2014th ed. Geneva, Switzerland: Group on Earth Observations; 2013. 164 p.

[39] Wulder MA, Kurz WA, Gillis M. National level forest monitoring and modeling in Canada. Prog Plann [Internet]. 2004 May [cited 2014 Mar 12];61(4):365–81. Available from: http://linkinghub.elsevier.com/retrieve/pii/S0305900603000692

[40] Nadkarni NM, Parker GG, Rinker HB, Jarzen DM. The nature of forest canopies. In: Lowman M, Rinker B, editors. Forest Canopies. second edition. Sarasota, Florida: Elsevier Inc.; 2004. p. 517.

[41] Sexton JO, Song X-P, Feng M, Noojipady P, Anand A, Huang C, et al. Global, 30-m resolution continuous fields of tree cover: landsat-based rescaling of MODIS vegetation

continuous fields with lidar-based estimates of error. Int J Digit Earth [Internet]. Taylor & Francis; 2013 Sep [cited 2014 Feb 13];6(5):427–48. Available from: http://www.tandfonline.com/doi/abs/10.1080/17538947.2013.786146

[42] Nandy S, Kushwaha SPS, Dadhwal VK. Forest degradation assessment in the upper catchment of the river Tons using remote sensing and GIS. Ecol Indic [Internet]. Elsevier Ltd; 2011 Mar [cited 2014 Feb 20];11(2):509–13. Available from: http://linkinghub.elsevier.com/retrieve/pii/S1470160X10001299

[43] Deutscher J, Perko R, Gutjahr K, Hirschmugl M, Schardt M. Mapping tropical rainforest canopy disturbances in 3D by COSMO-SkyMed spotlight InSAR-Stereo data to detect areas of forest degradation. Remote Sens [Internet]. 2013 Feb 4 [cited 2014 Mar 1];5(2): 648–63. Available from: http://www.mdpi.com/2072-4292/5/2/648/

[44] Souza, Jr C, Siqueira J, Sales M, Fonseca A, Ribeiro J, Numata I, et al. Ten-year landsat classification of deforestation and forest degradation in the Brazilian Amazon. Remote Sens [Internet]. 2013 Oct 28 [cited 2014 Feb 25];5(11):5493–513. Available from: http://www.mdpi.com/2072-4292/5/11/5493/

[45] Lu L, Li X, Veroustraete F, Kang E, Wang J. Analysing the forcing mechanisms for net primary productivity changes in the Heihe River Basin, north-west China. Int J Remote Sens [Internet]. 2009 [cited 2014 Mar 12];30(3):793–816. Available from: http://www.tandfonline.com/doi/abs/10.1080/01431160802438530

[46] Huang N, Niu Z, Wu C, Tappert MC. Modeling net primary production of a fast-growing forest using a light use efficiency model. Ecol Modell [Internet]. Elsevier B.V.; 2010 Dec [cited 2014 Mar 12];221(24):2938–48. Available from: http://linkinghub.elsevier.com/retrieve/pii/S0304380010004552

[47] Seaquist JW, Olsson L, Ardö J. A remote sensing-based primary production model for grassland biomes. Ecol Modell. 2003;169:131–55.

[48] Running SW, Nemani RR, Heinsch FA, Zhao M, Reeves M, Hashimoto H. A continuous satellite-derived measure of global terrestrial primary production [Internet]. BioScience. 2004. p. 547. Available from: http://www.jstor.org/stable/3333948

[49] Bai Z, Dent D, Olsson L, Schaepman M. Global assessment of land degradation and improvement. 1. Identification by remote sensing [Internet]. … Soil Reference and Information …. 2008. Available from: http://www.isric.nl/ISRIC/webdocs/docs/report 2008_01_glada international_rev_aug 2008.pdf

[50] Romero-Sanchez ME, Ponce-Hernandez R. The assessment of forest degradation in dry forested lands: mapping regional trend indicators of degradation in the Yucatan Peninsula, Mexico with satellite data. In: Hubert B, Broin M, editors. 3rd UNCCD Scienitific Conference: "Combating desertification/land degradation and drought for poverty reduction and sustainable development: the contribution of science, technology, traditional knowledge and practices". Montpelier, France: Agropolis International; 2015. pp. 284–5.

[51] Monteith JL. Solar radiation and productivity in tropical ecosystems. J Appl Ecol. 1972; 9:747-766.

[52] Verstraeten WW, Veroustraete F, Feyen J. On temperature and water limitation of net ecosystem productivity: implementation in the C-Fix model. Ecol Modell [Internet]. 2006 Nov [cited 2014 Mar 12];199(1):4–22. Available from: http://linkinghub.elsevier.com/retrieve/pii/S0304380006002778

[53] McCallum I, Wagner W, Schmullius C, Shvidenko A, Obersteiner M, Fritz S, et al. Satellite-based terrestrial production efficiency modeling. Carbon Balance Manag [Internet]. 2009 Jan [cited 2014 Jan 23];4:8. Available from: http://www.pubmedcentral.nih.gov/articlerender.fcgi?artid=2754440&tool=pmcentrez&rendertype=abstract

[54] Li S. Monitoring of Net Primary Production in California rangelands using landsat and MODIS satellite remote sensing. Nat Resour [Internet]. 2012 [cited 2014 Mar 5];03(02): 56–65. Available from: http://www.scirp.org/journal/PaperDownload.aspx?DOI=10.4236/nr.2012.32009

[55] Veroustraete F. On the use of a simple deciduous forest model for the interpretation of climate change effects at the level of carbon dynamics. Ecol Modell [Internet]. 1994 Sep [cited 2015 Jan 7];75–76:221–37. Available from: http://linkinghub.elsevier.com/retrieve/pii/0304380094900213

[56] Sabbe H, Veroustraete F. Estimation of net primary and net ecosystem productivity of European terrestrial ecosystems by means of the C-Fix model and NOAA / AVHRR data. 1996;1990(April 1992).

[57] Veroustraete F, Sabbe H, Eerens H. Estimation of carbon mass fluxes over Europe using the C-Fix model and Euroflux data. Remote Sens Environ [Internet]. 2002 Dec;83(3): 376–99. Available from: http://linkinghub.elsevier.com/retrieve/pii/S0034425702000433

[58] Ponce-Hernandez R, Ahmed OS. An approach to the assessment of historic trends of land degradation indicators at national scales: use of MODIS and AVHRR coarse resolution vegetation products for mapping in Ethiopia. In: Hubert B, Broin M, editors. 3rd UNCCD Scienitific Conference: "Combating desertification/land degradation and drought for poverty reduction and sustainable development: the contribution of science, technology, traditional knowledge and practices". Montpelier, France: Agropolis International; 2015. p. 277–8.

[59] Wulder MA, White JC, Goward SN, Masek JG, Irons JR, Herold M, et al. Landsat continuity: issues and opportunities for land cover monitoring. Remote Sens Environ [Internet]. 2008 Mar [cited 2014 Feb 21];112(3):955–69. Available from: http://linkinghub.elsevier.com/retrieve/pii/S0034425707003331

[60] Hansen M, Loveland T. A review of large area monitoring of land cover change using Landsat data. Remote Sens Environ [Internet]. Elsevier Inc.; 2012 Jul [cited 2014 Jan 20]; 122:1–9. Available from: http://linkinghub.elsevier.com/retrieve/pii/

S0034425712000314\nhttp://www.sciencedirect.com/science/article/pii/S0034425712000314

[61] Kennedy RE, Yang Z, Cohen WB. Detecting trends in forest disturbance and recovery using yearly Landsat time series: 1. LandTrendr — Temporal segmentation algorithms. Remote Sens Environ [Internet]. Elsevier Inc.; 2010 Dec 15 [cited 2014 Jan 20];114(12): 2897–910. Available from: http://linkinghub.elsevier.com/retrieve/pii/S0034425710002245

[62] Pflugmacher D, Cohen WB, Kennedy RE. Using Landsat-derived disturbance history (1972–2010) to predict current forest structure. Remote Sens Environ [Internet]. 2012 Jul [cited 2014 Feb 21];122:146–65. Available from: http://linkinghub.elsevier.com/retrieve/pii/S0034425712000533

[63] DeVries B, Verbesselt J, Kooistra L, Herold M. Robust monitoring of small-scale forest disturbances in a tropical montane forest using Landsat time series. Remote Sens Environ [Internet]. Elsevier Inc.; 2015; Available from: http://linkinghub.elsevier.com/retrieve/pii/S0034425715000656

[64] Lhermitte S, Verbesselt J, Verstraeten WW, Coppin P. A comparison of time series similarity measures for classification and change detection of ecosystem dynamics. Remote Sens Environ [Internet]. 2011 Dec [cited 2014 May 24];115(12):3129–52. Available from: http://linkinghub.elsevier.com/retrieve/pii/S0034425711002446

[65] Hilker T, Wulder MA, Coops NC, Seitz N, White JC, Gao F, et al. Generation of dense time series synthetic Landsat data through data blending with MODIS using a spatial and temporal adaptive reflectance fusion model. Remote Sens Environ [Internet]. 2009 Sep [cited 2014 Feb 26];113(9):1988–99. Available from: http://linkinghub.elsevier.com/retrieve/pii/S0034425709001709

[66] Upadhyay TP, Sankhayan PL, Solberg B. A review of carbon sequestration dynamics in the Himalayan region as a function of land-use change and forest/soil degradation with special reference to Nepal. Agric Ecosyst Environ [Internet]. 2005 Feb [cited 2014 Feb 20];105(3):449–65. Available from: http://linkinghub.elsevier.com/retrieve/pii/S0167880904002865

[67] Zhu Z, Woodcock CE, Olofsson P. Continuous monitoring of forest disturbance using all available Landsat imagery. Remote Sens Environ [Internet]. Elsevier Inc.; 2012 Jul [cited 2014 Jan 20];122:75–91. Available from: http://linkinghub.elsevier.com/retrieve/pii/S0034425712000387

[68] Kennedy RE, Cohen WB, Schroeder TA. Trajectory-based change detection for automated characterization of forest disturbance dynamics. Remote Sens Environ [Internet]. 2007 Oct [cited 2014 Mar 24];110(3):370–86. Available from: http://linkinghub.elsevier.com/retrieve/pii/S0034425707001216

[69] Cohen WB, Yang Z, Kennedy R. Detecting trends in forest disturbance and recovery using yearly Landsat time series: 2. TimeSync — Tools for calibration and validation.

Remote Sens Environ [Internet]. Elsevier B.V.; 2010 Dec 15 [cited 2014 Feb 25];114(12): 2911–24. Available from: http://linkinghub.elsevier.com/retrieve/pii/S0034425710002269

[70] Hussain M, Chen D, Cheng A, Wei H, Stanley D. Change detection from remotely sensed images: from pixel-based to object-based approaches. ISPRS J Photogramm Remote Sens [Internet]. International Society for Photogrammetry and Remote Sensing, Inc. (ISPRS); 2013;80:91–106. Available from: http://dx.doi.org/10.1016/j.isprsjprs.2013.03.006

[71] Lu D, Mausel P, Brondízio E, Moran E. Change detection techniques. Int J Remote Sens [Internet]. 2004 Jun [cited 2014 Jul 21];25(12):2365–401. Available from: http://www.tandfonline.com/doi/abs/10.1080/0143116031000139863

[72] CONAFOR, Chapingo UA. Land Degradation and Desertification baseline: Final report. Jalisco, Mexico. 2014.

[73] CONAFOR. National system of forest information: national forest and soils inventory. [Internet]. 2012. Available from: http://www.cnf.gob.mx:8080/snif/portal/infys

[74] Ju J, Roy DP. The availability of cloud-free Landsat ETM+ data over the conterminous United States and globally. Remote Sens Environ [Internet]. 2008 Mar [cited 2014 Apr 17];112(3):1196–211. Available from: http://linkinghub.elsevier.com/retrieve/pii/S0034425707004002

[75] Masek JG, Vermote EF, Saleous NE, Wolfe R, Hall FG, Huemmrich KF, et al. A Landsat surface reflectance dataset for North America, 1990–2000. IEEE Geosci Remote Sens Lett [Internet]. 2006 Jan [cited 2014 Apr 29];3(1):68–72. Available from: http://ieeexplore.ieee.org/lpdocs/epic03/wrapper.htm?arnumber=1576692

[76] Zhu X, Liu D, Chen J. A new geostatistical approach for filling gaps in Landsat ETM+ SLC-off images. Remote Sens Environ [Internet]. 2012 Sep [cited 2014 Jan 28];124:49–60. Available from: http://linkinghub.elsevier.com/retrieve/pii/S0034425712001952

[77] Romero-Sanchez ME, Ponce-Hernandez R, Franklin SE, Aguirre-Salado CA. Comparison of data gap-filling methods for Landsat ETM+ SLC-off imagery for monitoring forest degradation in a semi-deciduous tropical forest in Mexico. Int J Remote Sens [Internet]. 2015;36(11):2786–99. Available from: http://www.tandfonline.com/doi/full/10.1080/01431161.2015.1047991

[78] Asner GP. Automated mapping of tropical deforestation and forest degradation: CLASlite. J Appl Remote Sens [Internet]. 2009 Aug 1 [cited 2014 Jan 20];3(1):033543. Available from: http://remotesensing.spiedigitallibrary.org/article.aspx?doi=10.1117/1.3223675

[79] Asner GP, Heidebrecht KB. Spectral unmixing of vegetation, soil and dry carbon in arid regions: comparing multispectral and hyperspectral observations. Int J Remote Sens. 2002;23(19):3939–58.

[80] Asner GP, Keller M, Pereira R, Zweede JC, Jose N, Silva M. Canopy damage and recovery after selective logging in Amazonia: field and satellite studies. Ecol Appl. 2004;14(4):280–98.

[81] Smith AMS, Falkowski MJ, Hudak AT, Evans JS, Robinson AP, Steele CM. A cross-comparison of field, spectral, and lidar estimates of forest canopy cover. Can J Remote Sens. 2009;35(5):447–59.

[82] Ahmed OS, Franklin SE, Wulder MA. Integration of Lidar and Landsat data to estimate forest canopy cover in Coastal British Columbia. Photogramm Eng Remote Sens [Internet]. 2014 Oct 1 [cited 2015 Jan 15];80(10):953–61. Available from: http://essential.metapress.com/openurl.asp?genre=article&id=doi:10.14358/PERS.80.10.953

[83] Yuan W, Liu S, Zhou G, Zhou G, Tieszen LL, Baldocchi D, et al. Deriving a light use efficiency model from eddy covariance flux data for predicting daily gross primary production across biomes. Agric For Meteorol. 2007;143(3–4):189–207.

[84] Running SW, Thornton PE, Nemani RR, Glassy JM. Global terrestrial gross and net primary productivity from the earth observating system. In: Sala OE, Jackson RB, Mooney HA, Howart RW, editors. Methods in ecosystem science. Springer New York; 2000. p. 44–57.

[85] Running SW, Nemani R, Glassy JM, Thornton PE. Modis Daily Photosynthesis (Psn) and Annual Net Primary Production (Npp) Product. Report. Oak Ridge, Tennessee, USA.; 1999. 1-59.

[86] Raich JW, Rastetter EB, Melillo JM, Kicklighter DW, Steudler PA, Peterson BJ, et al. Potential net primary productivity in South America: application of a global model. Ecol Appl [Internet]. 1991;1(4):399–429. Available from: http://www.jstor.org/stable/1941899

[87] Medina E, Klinge H. Productivity of tropical forests and tropical woodlands. In: Lange O., Nobel PS, Osmond CB, Ziegler H, editors. Physiological Plant Ecology IV [Internet]. New York, NY: Springer Berlin Heidelberg; 1983. pp. 281–303. Available from: http://link.springer.com/chapter/10.1007/978-3-642-68156-1_10

[88] Xiao X, Hollinger D, Aber J, Goltz M, Davidson E a., Zhang Q, et al. Satellite-based modeling of gross primary production in an evergreen needleleaf forest. Remote Sens Environ. 2004;89(4):519–34.

[89] Verbesselt J, Zeileis A, Herold M. Near real-time disturbance detection using satellite image time series. Remote Sens Environ [Internet]. Elsevier Inc.; 2012 Aug [cited 2014 Mar 3];123:98–108. Available from: http://linkinghub.elsevier.com/retrieve/pii/S0034425712001150

[90] Gao J. Digital Analysis of Remotely Sensed Imagery. New York, NY: McGraw-Hill; 2009.

[91] Otsu N. A Threshold selection method from gray-level histograms. IEEE Trans Syst Man Cybern [Internet]. 1979;9(1):62–6. Available from: http://ieeexplore.ieee.org/stamp/stamp.jsp?arnumber=4310076

[92] Prieto-Blanco A, North PRJ, Barnsley MJ, Fox N. Satellite-driven modelling of Net Primary Productivity (NPP): theoretical analysis. Remote Sens Environ [Internet]. Elsevier Inc.; 2009 Jan [cited 2014 Feb 7];113(1):137–47. Available from: http://linkinghub.elsevier.com/retrieve/pii/S0034425708002708

[93] Wang L, Gong W, Ma Y, Zhang M. Modeling regional vegetation NPP variations and their relationships with climatic parameters in Wuhan, China. Earth Interact. 2013;17(4):1-20.

[94] Ruimy A, Kergoat L, Bondeau A, Intercomparison TP of the PNPPM. Comparing global models of terrestrial net primary productivity (NPP): analysis of differences in light absorption and light use efficiency. Glob Chang Biol. 1999;5:56–65.